

## A simple systematic design of phenylcarbazole derivatives for host materials to high-efficiency phosphorescent organic light-emitting diodes†

Cite this: *J. Mater. Chem. C*, 2013, **1**, 3967

Lin-Song Cui, Shou-Cheng Dong, Yuan Liu, Qian Li, Zuo-Quan Jiang\* and Liang-Sheng Liao\*

A series of novel blue phosphorescent host materials, namely, CTP-1, CTP-2 and CTP-3 have been designed and synthesized through the Suzuki–Miyaura cross-coupling reaction between *N*-phenylcarbazole and biphenyl. Their thermal, photophysical and electrochemical properties were systematically investigated. These novel hosts show excellent thermal stability and high glass transition temperatures ( $T_g$ ) ranging from 113 to 127 °C. The triplet energies of these three materials are significantly higher than that of (4,4'-bis(*N*-carbazolyl)-2,2'-biphenyl) (CBP, 2.56 eV) and that of the most popular blue phosphorescent material iridium(III) bis[(4,6-difluorophenyl)pyridinato-*N,C*<sup>2'</sup>] picolinate (Flrpic, 2.65 eV). These three novel materials have superior thermal and electronic properties for blue and white phosphorescent OLEDs. Blue emitting devices with an Ir-complex Flrpic as the phosphorescent dopant have been fabricated and show high efficiency with low roll-off. In particular, 40.4 cd A<sup>-1</sup> at 100 cd m<sup>-2</sup> and 38.2 cd A<sup>-1</sup> at 1000 cd m<sup>-2</sup> were achieved when CTP-1 was used as the host material. On the basis of this work, an all-phosphor white device with a current efficiency of 64.5 cd A<sup>-1</sup> at 100 cd m<sup>-2</sup> and 61.9 cd A<sup>-1</sup> at 1000 cd m<sup>-2</sup> has also been fabricated.

Received 5th March 2013

Accepted 17th April 2013

DOI: 10.1039/c3tc30410h

[www.rsc.org/MaterialsC](http://www.rsc.org/MaterialsC)

### Introduction

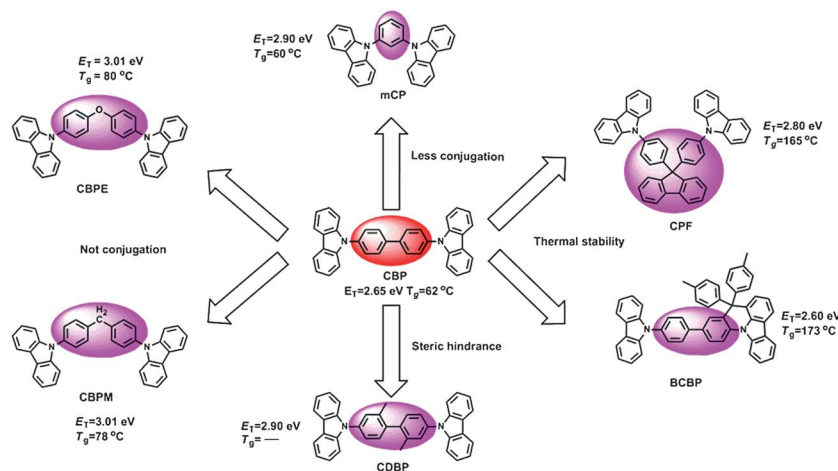
OLEDs, an abbreviation of Organic Light-Emitting Diodes, have broken through in the past decades, and they have been put into a wide range of applications in MP3 players, smartphones and cameras since 2003 because of their slimness and power-saving features. At the same time, OLED-based lighting is considered as another attractive application in future markets, although these products consist almost entirely of luxury lighting presently.<sup>1–5</sup> All of the progress can be traced back to the invention of phosphorescent OLEDs (PHOLEDs) in 1998,<sup>6,7</sup> which shed a new light on OLED technology and now it is widely accepted that only the use of PHOLEDs will enable the devices to achieve theoretical 100% internal quantum efficiencies.

To approach the target of high efficiency, phosphorescent emitters, which are usually composed of heavy metal complexes, should be doped into host materials by which the exciton's triplet–triplet annihilation (TTA) and triplet polaron quenching (TPQ) could thus be suppressed at a low concentration.<sup>8</sup> As we know, the host material reported in 1998 was

the CBP (4,4'-bis(*N*-carbazolyl)-2,2'-biphenyl) molecule which consists of two carbazole moieties and a biphenyl group and its concise synthetic route makes it widely used in today's research (Scheme 1).<sup>7</sup> Although numerous host materials have been developed to date, the carbazole derivatives are still the most favorable materials for chemists, because the derivatives can be readily tailored to fulfil the requirements for designing a good host, *e.g.* high triplet energy level, good thermal stability, appropriate transport mobility and matched HOMO and LUMO levels.<sup>9–19</sup> Despite the success of the CBP molecule in green or red PHOLEDs, for instance, the CBP itself possesses a low triplet energy of 2.56 eV, which severely limits its application in the most important blue PHOLEDs. In addition, its low glass-transition temperature of 78 °C may also undermine the device's operational stability. Hence, a series of modifications have been conducted to handle these disadvantages of CBP. In 2003, another classic host material mCP was reported with a high triplet energy (2.90 eV) by removing one phenyl group and modifying two carbazole moieties at the *meta*-linkage instead of the *para*-linkage, the power efficiency of the device hosted by mCP increased to 8.9 lm W<sup>-1</sup>.<sup>20</sup> In a similar way, Gong *et al.* designed and synthesized CBP isomers as blue host materials with high  $E_T$  and achieved good power efficiency.<sup>21</sup> Another approach to promote the triplet energy of CBP-based materials is by incorporating the steric effect to the molecular design. For example, CDBP and CPD use methyl groups as steric effect groups, and device power efficiencies arrived at 10.5 and 8.3 lm

Jiangsu Key Laboratory for Carbon-Based Functional Materials & Devices, Institute of Functional Nano & Soft Materials (FUNSOM), Soochow University, Suzhou, Jiangsu 215123, China. E-mail: zqjiang@suda.edu.cn; lsiao@suda.edu.cn; Fax: +86-65882846; Tel: +86-512-65880945

† Electronic supplementary information (ESI) available. See DOI: 10.1039/c3tc30410h



Scheme 1 CBP analogues host materials.

$W^{-1}$  respectively.<sup>22,23</sup> Interrupting the conjugation is also an effective strategy to raise the triplet energy. He *et al.* developed a series of non-conjugated carbazole hosts based on CBP, but the power efficiencies were moderate.<sup>13</sup> On the other hand, to overcome the thermal disadvantages of CBP, the molecular size should be enlarged. Noticeably, this molecular design must be carefully modulated, for the extent of conjugation is highly correlated with maintaining the triplet energy. A feasible means to solve this tradeoff is the introduction of a bulky group in the  $sp^3$ -hybridized linkage. For example, Jiang *et al.* used this linkage to bridge one *N*-phenylcarbazole moiety of CBP and Li *et al.* used this linkage to connect two *N*-phenylcarbazole moieties of CBP, and subsequently, high glass-transition temperatures ( $T_g$ ) were obtained for these materials.<sup>24,25</sup> However, it is reported that the increased distance resulted from these bulky groups may separate the conducting units from each other and lead to a lower carrier mobility.<sup>26</sup> Thus, in general, a rational molecular design is needed to face the dilemma among the sufficient triplet energy, the high morphological stability and the suitable carrier mobility of a host material.

In this work, we report the design and syntheses of three new carbazole-based materials CTP-1, CTP-2 and CTP-3. All of them are comprised of biphenyl and *N*-phenylcarbazole units and could be quite simply prepared in one-step. By altering the linking positions, these materials exhibited obvious differences in device performance. Their electrical, thermal and photo-physical properties were investigated. With regards to the aspect of molecular size, these new materials just add one more biphenyl group, as compared with the CBP molecule. Due to the *meta*-linkage, the triplet energies do not reduce but increase. The enlarged molecular size could also lead to the increased  $T_g$  of these materials. Blue PHOLEDs containing CTP-1, CTP-2, and CTP-3 as hosts and FIrpic as a dopant exhibited excellent efficiency performances with low roll-off. In particular, the device with CTP-1 as the host material showed the highest current efficiency of  $40.4 \text{ cd A}^{-1}$  at  $100 \text{ cd m}^{-2}$  and  $38.2 \text{ cd A}^{-1}$  at  $1000 \text{ cd m}^{-2}$  among the tested devices, which could possibly be

attributed to its best hole mobility and most sufficient energy transfer, as compared with the other two analogues. Meanwhile, the all-phosphor white devices hosted by these three materials were also fabricated and current efficiencies of  $64.5 \text{ cd A}^{-1}$  at  $100 \text{ cd m}^{-2}$ ,  $61.9 \text{ cd A}^{-1}$  at  $1000 \text{ cd m}^{-2}$  were achieved by using CTP-1 as the host material.

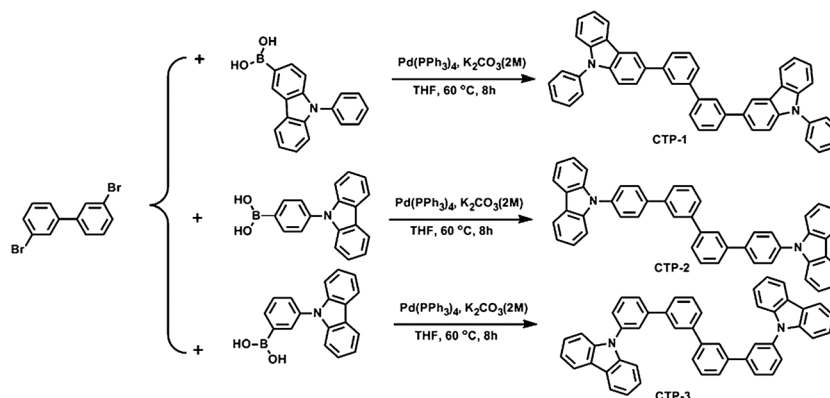
## Results and discussion

### Synthesis and characterization

The synthetic routes and chemical structures of the novel hosts are shown in Scheme 2. Three phenylcarbazole derivatives were readily prepared through a classic Suzuki–Miyaura cross-coupling reaction from 3,3'-dibromodiphenyl with the corresponding *N*-phenylcarbazole-3-boronic acid in high yields. Detailed synthetic procedures are presented in the Experimental section. Afterwards, all the target materials were further purified by repeated temperature gradient vacuum sublimation. The chemical structures of the target compounds were fully characterized by  $^1\text{H}$  NMR and  $^{13}\text{C}$  NMR spectroscopy, mass spectrometry and elemental analysis.

### Thermal properties

To confirm their thermal stabilities, these three compounds were investigated with thermogravimetric analysis (TGA) and differential scanning calorimetry (DSC) in a nitrogen atmosphere at a scanning rate of  $10 \text{ }^\circ\text{C min}^{-1}$  (Fig. 1). The three materials exhibited high thermal decomposition temperatures ( $T_d$ , corresponding to 5% weight loss, see Fig. S1†)  $448 \text{ }^\circ\text{C}$  for CTP-1,  $429 \text{ }^\circ\text{C}$  for CTP-2 and  $452 \text{ }^\circ\text{C}$  for CTP-3. Their glass-transition temperatures were observed at  $123 \text{ }^\circ\text{C}$  for CTP-1,  $127 \text{ }^\circ\text{C}$  for CTP-2 and  $113 \text{ }^\circ\text{C}$  for CTP-3, which are substantially higher than those of CBP-based derivative host materials, such as CBP ( $62 \text{ }^\circ\text{C}$ ), *m*-CBP ( $60 \text{ }^\circ\text{C}$ ), *o*-CBP ( $82 \text{ }^\circ\text{C}$ ) and CDBP ( $94 \text{ }^\circ\text{C}$ ). Therefore these three novel hosts show excellent thermal and morphological stability. The high  $T_g$  may be attributed to the extended molecular structure.



**Scheme 2** Synthetic routes and chemical structures of the host materials.

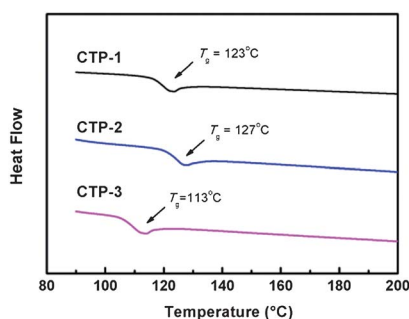


**Fig. 1** DSC traces recorded at a heating rate of 10 °C min<sup>-1</sup>.

### Photophysical properties

Fig. 2 depicts the electronic absorption and emission photoluminescence (PL) of CTP-1, CTP-2 and CTP-3 in CH<sub>2</sub>Cl<sub>2</sub> solution at room temperature. The absorption peaks at around 300 nm of the three materials are associated with the carbazole unit's  $\pi$ - $\pi^*$  transitions. The absorption in the range of 315 nm to 352 nm can be assigned to the  $\pi$ - $\pi^*$  transition between the carbazole moiety to its adjacent phenyl unit on the molecule. The intensity of the  $\pi$ - $\pi^*$  transitions is significantly reduced in comparison with that of CBP, which could be ascribed to the *meta*-conjugation for CTP-1, CTP-2 and CTP-3 instead of the *para*-linkage.<sup>27</sup>

Compounds CTP-1, CTP-2 and CTP-3 exhibit deep blue emissions with vibronic peaks located in the range 350–382 nm in CH<sub>2</sub>Cl<sub>2</sub> solution. The optical energy bandgaps ( $E_g$ ) of CTP-1, CTP-2 and CTP-3 are 3.49, 3.56, and 3.55 eV, respectively, which were calculated from the threshold of the absorption spectra in CH<sub>2</sub>Cl<sub>2</sub> solution. The phosphorescence spectra were measured in frozen 2-methyltetrahydrofuran matrix at 77 K, and the  $E_T$  values calculated from the spectra followed the sequence CTP-2 (2.73 eV) < CTP-1 (2.75 eV) < CTP-3 (2.81 eV). All the novel hosts exhibited higher  $E_T$  levels than those of CBP (2.64 eV) and the blue phosphor FIrpic (2.65 eV). Thus they can probably serve as good host materials for blue triplet emitters while CBP cannot due to its close  $E_T$  to that of the guest.

### Electrochemical properties

The electrochemical properties of CTP-1, CTP-2 and CTP-3 probed by cyclic voltammetry (CV) are shown in Fig. 3. The measurements were performed in CH<sub>2</sub>Cl<sub>2</sub> with ferrocene as the internal reference. All compounds exhibited irreversible oxidation behaviors which could unambiguously be assigned to the oxidation of the carbazole units.

The HOMO energies were deduced from the onset of the oxidation potentials with regard to the energy level of ferrocene (4.8 eV below the vacuum). The HOMO levels of CTP-1, CTP-2 and CTP-3 were estimated as 5.96, 5.99 and 6.00 eV, respectively, which are similar to that of CBP (6.01 eV). The LUMO energy levels were calculated from the HOMO values

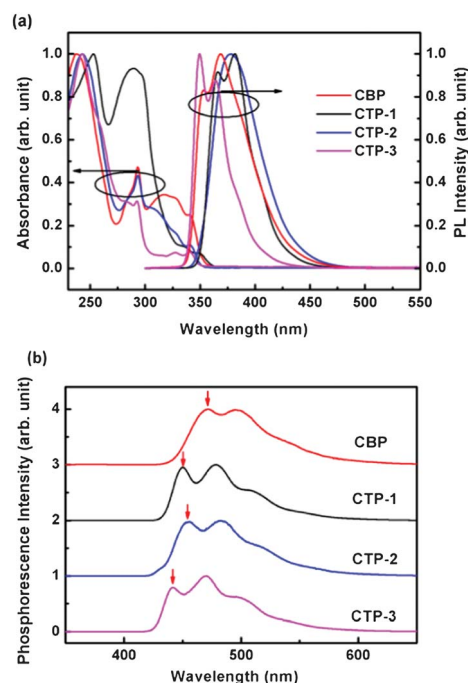


**Fig. 2** (a) UV-Vis absorption and PL spectra of CBP, CTP-1, CTP-2 and CTP-3 in dichloromethane solution at 10<sup>-5</sup> M. (b) Phosphorescence spectra of these compounds measured in a frozen 2-methyltetrahydrofuran matrix at 77 K. The arrows indicate the inferred triplet level positions.

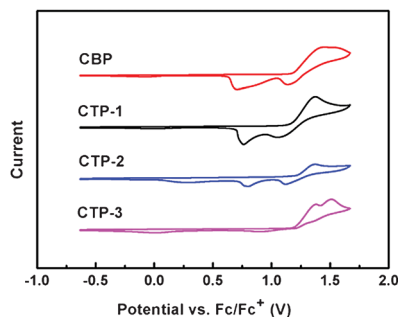


**Fig. 3** Cyclic voltammograms of CBP, CTP-1, CTP-2 and CTP-3 in dichloromethane solution for oxidation.

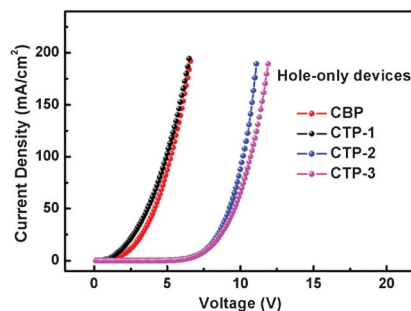


**Fig. 4** The current density–voltage ( $J$ – $V$ ) curves for the hole-only devices (ITO/MoO<sub>3</sub> (10 nm)/CBP, CTP-1, CTP-2 or CTP-3 (100 nm)/MoO<sub>3</sub> (10 nm)/Al (100 nm)).

and optical band gaps, and which were about 2.47, 2.43 and 2.45 eV, respectively. All the physical property data is summarized in Table 1.

### Hole transport properties

CBP possesses excellent hole transport mobility, which is much higher than that of the widely used electron transport material tris(8-hydroxyquinoline)aluminium (Alq<sub>3</sub>).<sup>28–30</sup> To evaluate the hole transport characters of these hosts, we fabricated hole-only devices with a device structure of ITO/MoO<sub>3</sub> (10 nm)/host (100 nm)/MoO<sub>3</sub> (10 nm)/Al (100 nm). The MoO<sub>3</sub> layer was utilized to prevent electron-injection from the cathode. Fig. 4 shows the current density *versus* voltage characteristics of the hole-only devices. Evidently, the hole mobility of the compound CTP-1 is slightly higher than that of CBP, but much higher than those of CTP-2 and CTP-3. These results could be supported by the molecular simulation. In the view of the structure from computational calculation, the HOMO of CTP-1 is distributed on the main chain composed of six phenyl rings, while the HOMOs of CTP-2 and CTP-3 are barely distributed on the peripheral carbazole rings. This is mainly attributed to the fact that the p-orbital on the nitrogen atom with two lone pairs of electrons could also participate in the conjugation and the phenyl rings at the biphenyl  $\pi$ -bridge locate at the *para*-position to the nitrogen (*e.g.* at the 3-position of carbazole), and which could give rise to longer effective conjugation on the HOMO (see Fig. S1†) and indicates better hole-mobility. In contrast, in the excited state, there is no empty orbital on the nitrogen atom and it cannot participate in the formation of the LUMO anymore,

and thus only the phenyl rings on the carbazole moiety occupy the LUMO while the ring at the  $\pi$ -bridge does not.

### Phosphorescent OLEDs

In order to evaluate the functioning of the novel materials for blue phosphorescent emitters, we fabricated PHOLEDs with typical sandwiched structures by sequential vapor deposition of the materials onto a glass substrate coated with ITO, the blue Ir-complex Firpic doped into the three hosts as the emitting layer. We utilized strongly electron-deficient 1,4,5,8,9,11-hexaaza-triphenylene-hexacarbonitrile (HAT-CN) as the hole-injection layer (HIL), 1,1-bis[4-*N,N*-di(*p*-tolyl)amino]phenyl]cyclohexane (TAPC) was used as the hole-transporting layer (HTL) and the electron-blocking layer. 1,3,5-tri[[3-pyridyl]-phen-3-yl]benzene (TmPyPB) was utilized as the electron-transporting as well as the hole-blocking layer. Liq. served as the electron-injecting layer and Al served as the cathode. The blue PHOLED's structures were ITO/HAT-CN (10 nm)/TAPC (45 nm)/Host: Firpic (8%, 20 nm)/TmPyPB (40 nm)/Liq. (2 nm)/Al (120 nm) (Host = CTP-1: device C; Host = CTP-2: device D; Host = CTP-3: device E). Meanwhile, the control devices using CBP (device A) and mCP (device B) as hosts were also fabricated. Fig. 5 depicts the relative energy levels of the materials employed in the devices.

The current density–voltage–luminance ( $J$ – $V$ – $L$ ) and efficiency *versus* current density curves for the devices are depicted in Fig. 6. All the OLED's performances are summarized in Table 2. As expected, the operating voltage of the devices at 100 cd m<sup>-2</sup> based on CTP-1 (3.8 eV) is lower than that of the devices based on CTP-2 (4.5 eV) and CTP-3 (4.6 eV), which is consistent with the hole-only device results observed in Fig. 4. This may be

**Table 1** Physical properties of CBP, CTP-1, CTP-2 and CTP-3

| Compound | $T_g^a$ (°C) | $T_d^a$ (°C) | $\lambda_{\text{abs}}^b$ (nm) | $\lambda_{\text{em}}^b$ (nm) | $\lambda_{\text{ph}}^c$ (nm) | $E_g^d$ (eV) | $E_T^e$ (eV) | HOMO/LUMO <sup>f</sup> (eV) |
|----------|--------------|--------------|-------------------------------|------------------------------|------------------------------|--------------|--------------|-----------------------------|
| CBP      | 62           | 283          | 293, 319                      | 378                          | 470                          | 3.40         | 2.64         | 6.01/2.61                   |
| CTP-1    | 123          | 448          | 288, 336                      | 365, 380                     | 448                          | 3.49         | 2.75         | 5.96/2.47                   |
| CTP-2    | 127          | 429          | 293, 305                      | 352, 368                     | 454                          | 3.56         | 2.73         | 5.99/2.43                   |
| CTP-3    | 113          | 452          | 292, 328                      | 349, 365                     | 441                          | 3.55         | 2.81         | 6.00/2.45                   |

<sup>a</sup>  $T_g$ : glass transition temperatures. <sup>b</sup> Measured in dichloromethane solution at room temperature. <sup>c</sup> Measured in 2-MeTHF glass matrix at 77 K. <sup>d</sup>  $E_g$ : the band gap energies were estimated from the optical absorption edges of the UV-Vis absorption spectra. <sup>e</sup>  $E_T$ : the triplet energy were estimated from the onset peak of the phosphorescence spectra. <sup>f</sup> HOMO and LUMO estimated from the onset of oxidation potentials and the optical band gap from the absorption spectra.

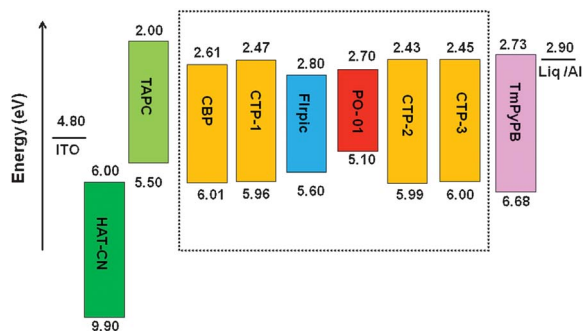


Fig. 5 Energy level diagrams for the devices.

due to the higher hole mobility of CTP-1 resulted from its relatively higher conjugation. As illustrated in Fig. 6, when operated at the luminance of  $100 \text{ cd m}^{-2}$ , device C hosted by CTP-1 exhibited the best performance with a current efficiency of  $40.4 \text{ cd A}^{-1}$  and a power efficiency of  $33.8 \text{ lm W}^{-1}$ ; while device D hosted by CTP-2 and device E hosted by CTP-3 exhibited  $36.9 \text{ cd A}^{-1}$  ( $25.6 \text{ lm W}^{-1}$ ) and  $37.4 \text{ cd A}^{-1}$  ( $25.5 \text{ lm W}^{-1}$ ), respectively. Remarkably, all the devices showed a low efficiency roll-off. For example, when the luminance reached  $1000 \text{ cd m}^{-2}$ , the current efficiency was still as high as  $38.2 \text{ cd A}^{-1}$  for device C. In comparison, the control device A/B hosted by CBP/mCP as the emitting layer showed a relatively poorer performance.

The EL spectra and the Commission International de l'Éclairage (CIE) coordinates vary very little for these devices. All the devices show identical spectra with a peak at  $476 \text{ nm}$  and a shoulder at  $500 \text{ nm}$ , which is arising from the typical emission of the phosphor FIrpic.

In addition, we were motivated to test the applicability of CTP-1, CTP-2 and CTP-3 for all the phosphor white OLEDs with the configuration of ITO/HAT-CN (10 nm)/TAPC (45 nm)/Host: FIrpic (8%, 19 nm)/Host: PO-01 (5%, 1 nm)/TmPyPB (40 nm)/Liq. (2 nm)/Al (120 nm) (Host = CTP-1: device F; Host = CTP-2: device G; Host = CTP-3: device H). Fig. 7 shows the  $J$ - $V$ - $L$  characteristics and curves of current efficiency, power efficiency and external quantum efficiency versus current density. The devices F-H obtained the maximum current efficiencies of  $64.5$ ,  $56.0$ ,  $60.0 \text{ cd A}^{-1}$  and the maximum power efficiencies of  $49.5$ ,  $37.1$ ,  $37.9 \text{ lm W}^{-1}$ , respectively. Moreover, the emission color of these devices exhibited stability and varied slightly from (0.34, 0.47) at 4 V to (0.35, 0.48) at 8 V. The detailed device performances are summarized in Table 2.

For the WOLEDs, the current/power efficiencies of the devices hosted by these materials are in the order device F > device J  $\approx$  device H. This data agrees well with the tendencies of the blue phosphorescence performance, which demonstrates the superiority of CTP-1.

To further verify the exciton confinement properties of the hosts, transient photoluminescence decays of thin films (formed on quartz substrates with a thickness of 40 nm) with 10 wt% FIrpic dispersed in CBP, CTP-1, CTP-2 and CTP-3 were measured. According to Fig. 8, the emission of FIrpic-doped CTP-1, CTP-2 and CTP-3 films display nearly mono-exponential decay curves, indicating that the triplet energy transfer from FIrpic to hosts is completely suppressed and the energy is well confined in emission layer. However the CBP: FIrpic film exhibited an unclear exponential curve with the lowest decay, indicating the insufficient energy transfer from CBP to FIrpic in the emission layer. This could be attributed to the

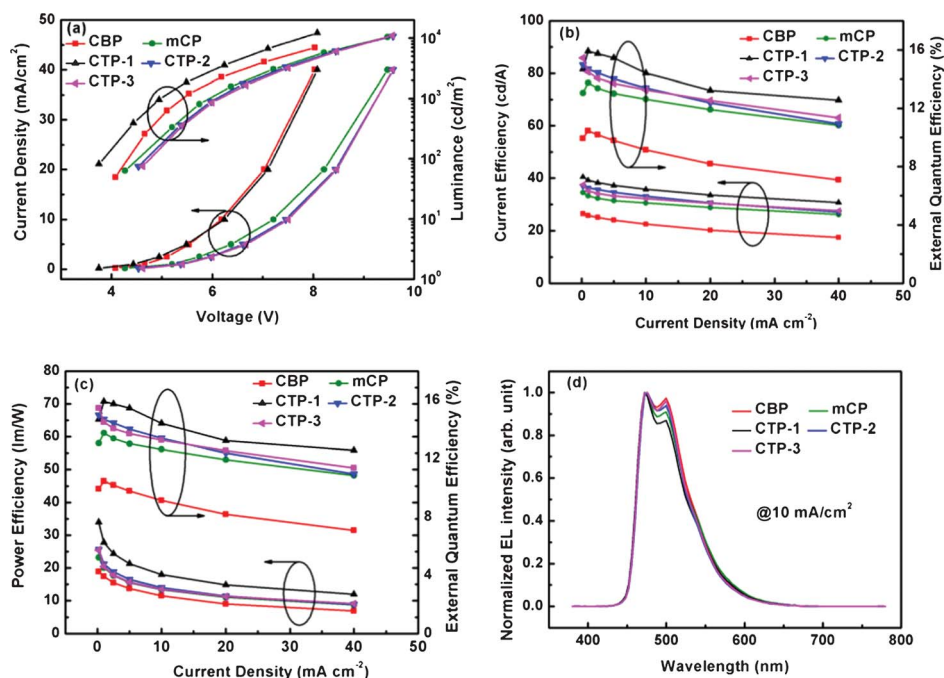


Fig. 6 (a) Current density–voltage–luminance characteristics, (b) current efficiency and external quantum efficiency versus current density curves, (c) power efficiency and external quantum efficiency versus current density curves, (d) the EL spectrum of devices A–E at  $10 \text{ mA cm}^{-2}$ .

**Table 2** Summary of OLED performances

| Device | Host/guest  | At 100 cd m <sup>-2</sup>                         |  | At 1000 cd m <sup>-2</sup> | $\eta_{c,max}/\eta_{p,max}/\eta_{ext,max}^b$<br>(cd/A/lm/W/%/V) |              | CIE (x,y) <sup>c</sup> |
|--------|-------------|---|--|----------------------------|---|--------------|------------------------|
|        |             | $\eta_c/\eta_p/\eta_{ext}/V^2$<br>(cd/A/lm/W/%/V) |  |                            |   |              |                        |
| A      | CBP/B       | 26.4/18.3/10.4/4.5                                |  | 24.4/14.4/9.78/5.3         | 26.5/18.8/10.4/4.0  | (0.17, 0.38) |                        |
| B      | mCP/B       | 34.3/22.8/13.7/4.7                                |  | 32.1/17.1/13.0/5.9         | 34.5/23.1/13.7/4.2  | (0.16, 0.38) |                        |
| C      | CTP-1/B     | 40.4/33.8/15.9/3.8                                |  | 38.2/24.2/15.7/4.9         | 40.5/33.9/15.9/3.7  | (0.16, 0.38) |                        |
| D      | CTP-2/B     | 36.9/25.6/14.7/4.5                                |  | 35.6/18.6/14.4/6.1         | 37.0/25.7/14.9/4.5  | (0.16, 0.39) |                        |
| E      | CTP-3/B     | 37.4/25.5/14.4/4.6                                |  | 34.1/17.9/13.7/6.2         | 37.5/25.6/15.4/4.6  | (0.17, 0.38) |                        |
| F      | CTP-1/B + Y | 64.5/49.5/19.1/4.0                                |  | 61.9/40.5/19.5/4.7         | 64.5/49.5/19.1/4.0  | (0.36, 0.48) |                        |
| G      | CTP-2/B + Y | 56.0/37.1/17.7/4.7                                |  | 47.5/24.7/15.0/6.0         | 56.0/37.1/17.7/4.7  | (0.35, 0.48) |                        |
| H      | CTP-3/B + Y | 60.0/37.9/18.9/4.9                                |  | 50.2/25.0/15.9/6.2         | 60.0/37.9/18.9/4.9  | (0.35, 0.48) |                        |

<sup>a</sup> Current efficiency ( $\eta_c$ ), power efficiency ( $\eta_p$ ), external quantum efficiency ( $\eta_{ext}$ ), voltage (V) at 100 cd m<sup>-2</sup> and 1000 cd m<sup>-2</sup>. <sup>b</sup> Maximum current efficiency ( $\eta_{c,max}$ ), maximum power efficiency ( $\eta_{p,max}$ ), maximum external quantum efficiency ( $\eta_{ext,max}$ ). <sup>c</sup> Measured at 10 mA cm<sup>-2</sup>.

close triplet energy level of CBP (2.64 eV) and Firpic (2.65 eV), which results in the diffusion of excitons out of the emissive layer and thus lowers the device performance. On the contrary, the CTP-1: Firpic film exhibited the quickest energy transfer, and this tendency is consistent with the device performance.

As outlined in the introduction, there is a dilemma in design among the high triplet energy, stable morphology, appropriate HOMO/LUMO levels for carrier injection and the high carrier transport mobility. Satisfactorily, CTP-1 could fulfill all the aspects proposed in the dilemma and in fact, according to the device performances, it could be utilized as a good host material, as compared to several representative CBP analogue host materials (Table 3).

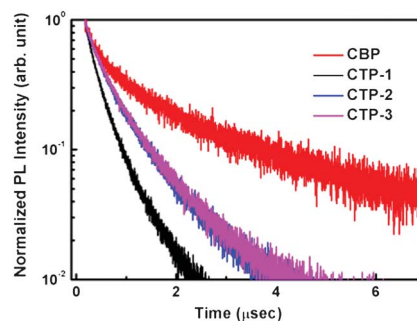


**Fig. 8** Transient photoluminescence decay (excited at 330 nm) curves at room temperature at 475 nm for the Firpic co-deposited with CBP, CTP-1, CTP-2 and CTP-3.

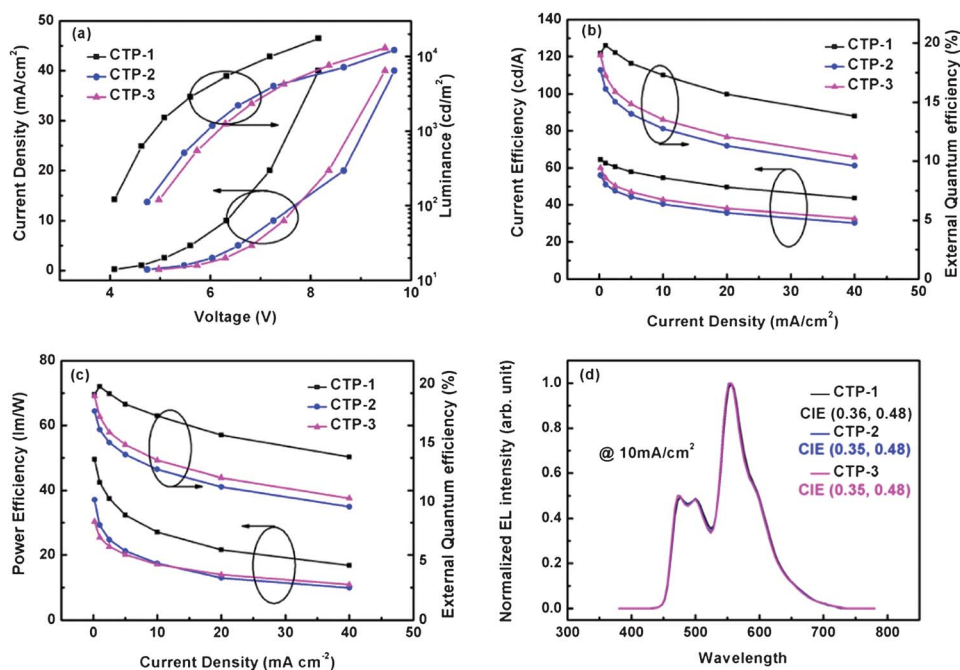


**Fig. 7** (a) Current density–voltage–luminance characteristics, (b) current efficiency and external quantum efficiency versus current density curves, (c) power efficiency and external quantum efficiency versus current density curves, (d) the EL spectrum of devices A–E at 10 mA cm<sup>-2</sup>.

**Table 3** Physical properties and device performances of the CBP analogue host materials

| Host          | $T_g$ (°C) | $E_T$ (eV) | Dopant        | $\eta_{\text{ext}}^a$ (%) | Ref.      |
|---------------|------------|------------|---------------|---------------------------|-----------|
| CBP           | 62         | 2.56       | <i>Flrpic</i> | 7.7                       | 33        |
| <i>mCP</i>    | 60         | 2.90       | <i>Flrpic</i> | 7.5                       | 34        |
| CDBP          | —          | 2.95       | <i>Flrpic</i> | 10.4                      | 22        |
| CPD           | —          | 3.02       | <i>Flrpic</i> | 8.7                       | 23        |
| CPF           | 165        | 2.88       | <i>Flrpic</i> | —                         | 25        |
| <i>o</i> -CBP | 82         | 3.00       | <i>Flrpic</i> | 14.2                      | 21        |
| 4CzPBP        | 120        | 2.80       | <i>Flrpic</i> | 14.5                      | 35        |
| BCBP          | 173        | 2.60       | <i>Flrpic</i> | 4.0                       | 24        |
| CTP-1         | 123        | 2.75       | <i>Flrpic</i> | 15.9                      | This work |
| CTP-2         | 127        | 2.73       | <i>Flrpic</i> | 14.9                      | This work |
| CTP-3         | 113        | 2.81       | <i>Flrpic</i> | 15.4                      | This work |

<sup>a</sup> Maximum external quantum efficiency.

## Conclusion

In conclusion, three novel light-emitting host materials (CTP-1, CTP-2 and CTP-3) comprised of biphenyl and *N*-phenylcarbazole have been developed. All the compounds could be afforded by a facile synthetic route. In view of the molecular design, to cope with the major challenge of having both a large enough triplet energy and acceptable morphological stability in a material, we simply added a biphenyl group and tried to vary the link-position of the *N*-phenylcarbazole moiety, which is unlike the other modification methods, such as “torsion”, “steric effect”, “conjugation interruption” and “bulky group”. Our methods effectively enlarged the molecular size and retained their triplet energies. Especially, the CTP-1 molecule possesses appropriate HOMO/LUMO levels, without sacrificing the carrier mobility by using *meta*-linkage to the carbazole rings. The computational calculation also indicates this way of linking could lead to effectively longer conjugation. These properties enable CTP-1 to be a good material in blue and white phosphorescent devices, and the blue light-emitting device exhibits  $40.4 \text{ cd A}^{-1}$  ( $33.8 \text{ lm W}^{-1}$ ) at  $100 \text{ cd m}^{-2}$  and  $38.2 \text{ cd A}^{-1}$  ( $24.2 \text{ lm W}^{-1}$ ) at  $1000 \text{ cd m}^{-2}$  with very low efficiency roll-off. Furthermore, the all-phosphor white device hosted by CTP-1 achieved a current efficiency of  $64.5 \text{ cd A}^{-1}$  ( $49.5 \text{ lm W}^{-1}$ ) at  $100 \text{ cd m}^{-2}$  and  $61.9 \text{ cd A}^{-1}$  ( $40.5 \text{ lm W}^{-1}$ ) at  $1000 \text{ cd m}^{-2}$ . These performances are believed to be among the best results as compared with other attempts in tailoring the CBP to be a better blue host material, indicating the simple modification could evidently overcome its intrinsic disadvantages and maintain its advantages simultaneously to achieve good performance.

## Experimental section

### Materials and methods

All the chemicals *i.e.*, (9-phenyl-9*H*-carbazol-3-yl) boronic acid, [4-(9*H*-carbazol-9-yl) phenyl] boronic acid, [3-(9*H*-carbazol-9-yl)-phenyl] boronic acid, 1-bromo-3-iodobenzene, 3-bromobenzenboronic acid were purchased from Bepharma limited and Alfa Aesar. All of the materials were used without further purification. The important intermediate 3,3'-dibromodiphenyl was prepared according to a literature method.<sup>31</sup> THF was purified

by the PURE SOLV (Innovative Technology) purification system. Chromatographic separations were carried out by using silica gel (200–300 nm). All other reagents were used as received from commercial sources unless otherwise stated. <sup>1</sup>H NMR and <sup>13</sup>C NMR spectra were recorded on a Varian Unity Inova 400 spectrometer at room temperature. Mass spectra were recorded on a Thermo ISQ mass spectrometer using a direct exposure probe. UV-Vis absorption spectra were recorded on a Perkin Elmer Lambda 750 spectrophotometer. PL spectra and phosphorescent spectra were recorded on a Hitachi F-4600 fluorescence spectrophotometer. Transient PL decays were measured by a single photon counting spectrometer from HORIBA JOBIN YVON with a Nano LED pulse lamp as the excitation source. Differential scanning calorimetry (DSC) was performed on a TA DSC 2010 unit at a heating rate of  $10 \text{ °C min}^{-1}$  under nitrogen. The glass transition temperatures ( $T_g$ ) were determined from the second heating scan. Thermogravimetric analysis (TGA) was performed on a TA SDT 2960 instrument at a heating rate of  $10 \text{ °C min}^{-1}$  under nitrogen. The temperature at 5% weight loss was used as the decomposition temperature ( $T_d$ ). Cyclic voltammetry (CV) was carried out on a CHI600 voltammetric analyzer at room temperature with a conventional three-electrode configuration consisting of a platinum disk working electrode, a platinum wire auxiliary electrode, and an Ag wire pseudo-reference electrode with ferrocenium/ferrocene ( $\text{Fc}^+/\text{Fc}$ ) as the internal standard. Nitrogen-purged dichloromethane was used as the solvent for the oxidation scan and DMF for the reduction scan with tetrabutylammonium hexafluorophosphate (TBAPF6) (0.1 M) as the supporting electrolyte. The cyclic voltammograms were obtained at a scan rate of  $100 \text{ mV s}^{-1}$ .

### Computational methodology

The geometrical and electronic properties of CTP-1, CTP-2 and CTP-3 were performed with the Gaussian 09 program package. The calculation was optimized by means of the wb97xd (Becke three parameters hybrid functional with Lee–Yang–Perdew correlation functionals) with the 6-31G(d) atomic basis set. Molecular orbitals were visualized using Gaussview.

### Fabrication of the OLEDs

The OLEDs were fabricated through vacuum deposition of the materials at *ca.*  $2 \times 10^{-6}$  Torr onto ITO-coated glass substrates having a sheet resistance of *ca.*  $30 \text{ } \Omega$  per square. The ITO surface was cleaned ultrasonically – sequentially with acetone, ethanol, and deionized water, then dried in an oven, and finally exposed to UV-ozone for about 30 min. Organic layers were deposited at a rate of  $2\text{--}3 \text{ } \text{Å s}^{-1}$ , subsequently, Liq. was deposited at  $0.2 \text{ } \text{Å s}^{-1}$  and then capped with Al (*ca.*  $4 \text{ } \text{Å s}^{-1}$ ) through a shadow mask without breaking the vacuum. For all the OLEDs, the emitting areas were determined by the overlap of two electrodes as  $0.09 \text{ cm}^2$ . The EL spectra, CIE coordinates and *J–V–L* curves of the devices were measured with a PHOTO RESEARCH SpectraScan PR 655 photometer and a KEITHLEY 2400 SourceMeter constant current source at room temperature. The EQE values were values that were calculated according to the previously reported methods.<sup>32</sup>

### General procedure for the Suzuki–Miyaura cross-coupling reaction

3,3'-Dibromodiphenyl (1 equiv.), carbazole-containing boronic acid (2.2 equiv.) and tetrakis(triphenylphosphine)palladium(0) (0.05 equiv.) were dissolved in THF/2 M K<sub>2</sub>CO<sub>3</sub> (3/1, v/v). The reaction mixture was heated to 60 °C for 8 h under an argon atmosphere. After cooling to room temperature, the organic layer was separated and evaporated to remove solvent. The residue was purified by column chromatography with 1 : 3 (v/v) dichloromethane/petroleum ether as the eluent and recrystallized from dichloromethane/petroleum and vacuum sublimation to give the final compound.

### Synthesis of CTP-1

3,3'-Dibromodiphenyl (1.50 g, 4.81 mmol), 9-phenyl-9H-carbazol-3-ylboronic acid (3.03 g, 10.56 mmol). The final product was a white crystalline powder (2.61 g, 85.5%). <sup>1</sup>H NMR (400 MHz, CDCl<sub>3</sub>) δ (ppm): 8.43 (s, 2H) 8.21 (d, *J* = 8.0 Hz, 2H) 8.03 (s, 2H) 7.76–7.70 (m, 4H) 7.68 (d, *J* = 8.0 Hz, 2H) 7.64–7.55 (m, 10H) 7.51–7.37 (m, 8H), 7.33–7.26 (m, 2H). <sup>13</sup>C NMR (400 MHz, CDCl<sub>3</sub>) δ (ppm): 142.6, 142.0, 141.4, 140.5, 137.6, 133.4, 129.9, 129.3, 129.9, 129.3, 127.5, 127.1, 126.5, 126.4, 126.2, 125.7, 125.6, 110.1, 109.9. MS (EI): *m/z* 636.52 [M<sup>+</sup>]. Anal. calcd for C<sub>48</sub>H<sub>32</sub>N<sub>2</sub> (%): C 90.54, H 5.07, N 4.40; found: C 90.54, H 5.50, N 4.46%.

### Synthesis of CTP-2

3,3'-Dibromodiphenyl (1.00 g, 3.21 mmol), [4-(9H-carbazol-9-yl)-phenyl] boronic acid (2.02 g, 7.06 mmol). The final product was a white powder (1.75 g, 86.0%). <sup>1</sup>H NMR (400 MHz, CDCl<sub>3</sub>) δ (ppm): 8.1 (s, 2H) 7.9 (s, 1H) 7.85 (d, *J* = 8.0 Hz, 2H) 7.69–7.53 (m, 5H) 2.14 (d, *J* = 8.0 Hz, 2H) 7.38–7.33 (m, 2H) 7.25–7.21 (m, 2H). <sup>13</sup>C NMR (400 MHz, CDCl<sub>3</sub>) 141.8, 140.8, 140.2, 137.1, 129.5, 128.6, 127.4, 126.6, 126.3, 125.9, 123.4, 120.3, 120.0. MS (EI): *m/z* 636.45 [M<sup>+</sup>]. Anal. calcd for C<sub>48</sub>H<sub>32</sub>N<sub>2</sub> (%): C 90.54, H 5.07, N 4.40; found: C 90.32, H 4.67, N 4.77%.

### Synthesis of CTP-3

3,3'-Dibromodiphenyl (1.00 g, 3.21 mmol), [4-(9H-carbazol-9-yl)-phenyl] boronic acid (2.02 g, 7.06 mmol). The final product was a white powder (1.79 g, 87.5%). <sup>1</sup>H NMR (400 MHz, CDCl<sub>3</sub>) δ (ppm): 8.15 (d, *J* = 8.0 Hz, 4H) 7.88 (d, *J* = 8.0 Hz, 4H) 7.74 (d, *J* = 8.0 Hz, 2H), 7.69–7.60 (m, 6H), 7.57–7.50 (m, 4H), 7.47 (d, *J* = 8.0 Hz, 4H), 7.42–7.36 (m, 4H), 7.31–7.24 (m, 4H). <sup>13</sup>C NMR (400 MHz, CDCl<sub>3</sub>) δ (ppm): 143.0, 141.8, 140.9, 140.8, 138.3, 130.3, 129.5, 126.8, 126.4, 126.3, 126.2, 126.0, 125.8, 123.4, 120.4, 120.0, 109.8. MS (EI): *m/z* 636.48 [M<sup>+</sup>]. Anal. calcd for C<sub>48</sub>H<sub>32</sub>N<sub>2</sub> (%): C 90.54, H 5.07, N 4.40; found: C 90.32, H 5.06, N 4.46%.

## Acknowledgements

We are grateful to the assistance of Dr Cheng Zhong in the molecular simulation. We acknowledge financial support from the Natural Science Foundation of China (no. 21202114, no. 21161160446, no. 61036009, and no. 61177016), the National High-Tech Research Development Program (no. 2011AA03A110),

and the Natural Science Foundation of Jiangsu Province (no. BK2010003). This was also a project funded by the Priority Academic Program Development of Jiangsu Higher Education Institutions (PAPD) and by the Research Supporting Program of Suzhou Industrial Park.

## Notes and references

- 1 S. Reineke, F. Lindner, G. Schwartz, N. Seidler, K. Walzer, B. Lussem and K. Leo, *Nature*, 2009, **459**, 234–238.
- 2 K. T. Kamtekar, A. P. Monkman and M. R. Bryce, *Adv. Mater.*, 2010, **22**, 572–582.
- 3 G. M. Farinola and R. Ragni, *Chem. Soc. Rev.*, 2011, **40**, 3467–3482.
- 4 M. C. Gather, A. Köhnen and K. Meerholz, *Adv. Mater.*, 2011, **23**, 233–248.
- 5 X.-H. Zhu, J. Peng, Y. Cao and J. Roncali, *Chem. Soc. Rev.*, 2011, **40**, 3509–3524.
- 6 M. A. Baldo, D. F. O'Brien, Y. You, A. Shoustikov, S. Sibley, M. E. Thompson and S. R. Forrest, *Nature*, 1998, **395**, 151–154.
- 7 M. A. Baldo, S. Lamansky, P. E. Burrows, M. E. Thompson and S. R. Forrest, *Appl. Phys. Lett.*, 1999, **75**, 4–6.
- 8 Y. Tao, C. Yang and J. Qin, *Chem. Soc. Rev.*, 2011, **40**, 2943–2970.
- 9 A. Chaskar, H.-F. Chen and K.-T. Wong, *Adv. Mater.*, 2011, **23**, 3876–3895.
- 10 K. Brunner, A. Van Dijken, H. Boerner, J. J. A. M. Bastiaansen, N. M. M. Kiggen and B. M. W. Langeveld, *J. Am. Chem. Soc.*, 2004, **126**, 6035–6042.
- 11 A. van Dijken, J. J. A. M. Bastiaansen, N. M. M. Kiggen, B. M. W. Langeveld, C. Rothe, A. Monkman, I. Bach, P. Stössel and K. Brunner, *J. Am. Chem. Soc.*, 2004, **126**, 7718–7727.
- 12 M.-H. Tsai, Y.-H. Hong, C.-H. Chang, H.-C. Su, C.-C. Wu, A. Matoliukstyte, J. Simokaitiene, S. Grigalevicius, J. V. Grazulevicius and C.-P. Hsu, *Adv. Mater.*, 2007, **19**, 862–866.
- 13 J. He, H. Liu, Y. Dai, X. Ou, J. Wang, S. Tao, X. Zhang, P. Wang and D. Ma, *J. Phys. Chem. C*, 2009, **113**, 6761–6767.
- 14 S. O. Jeon, K. S. Yook, C. W. Joo and J. Y. Lee, *Adv. Funct. Mater.*, 2009, **19**, 3644–3649.
- 15 Y.-M. Chen, W.-Y. Hung, H.-W. You, A. Chaskar, H.-C. Ting, H.-F. Chen, K.-T. Wong and Y.-H. Liu, *J. Mater. Chem.*, 2011, **21**, 14971–14978.
- 16 D. Kim, V. Coropceanu and J. L. Bredas, *J. Am. Chem. Soc.*, 2011, **133**, 17895–17900.
- 17 H. S. Son and J. Y. Lee, *Org. Electron.*, 2011, **12**, 1025–1032.
- 18 J. Li, T. Zhang, Y. Liang and R. Yang, *Adv. Funct. Mater.*, 2012, **23**, 619–628.
- 19 H. Sasabe, N. Toyota, H. Nakanishi, T. Ishizaka, Y.-J. Pu and J. Kido, *Adv. Mater.*, 2012, **24**, 3212–3217.
- 20 R. J. Holmes, S. R. Forrest, Y. J. Tung, R. C. Kwong, J. J. Brown, S. Garon and M. E. Thompson, *Appl. Phys. Lett.*, 2003, **82**, 2422–2424.
- 21 S. Gong, X. He, Y. Chen, Z. Jiang, C. Zhong, D. Ma, J. Qin and C. Yang, *J. Mater. Chem.*, 2012, **22**, 2894–2899.
- 22 S. Tokito, T. Iijima, Y. Suzuri, H. Kita, T. Tsuzuki and F. Sato, *Appl. Phys. Lett.*, 2003, **83**, 569–571.

- 23 L. Deng, X. Wang, Z. Zhang and J. Li, *J. Mater. Chem.*, 2012, **22**, 19700–19708.
- 24 Z. Jiang, X. Xu, Z. Zhang, C. Yang, Z. Liu, Y. Tao, J. Qin and D. Ma, *J. Mater. Chem.*, 2009, **19**, 7661–7665.
- 25 W. Li, J. Qiao, L. Duan, L. Wang and Y. Qiu, *Tetrahedron*, 2007, **63**, 10161–10168.
- 26 M. M. Rothmann, S. Haneder, E. Da Como, C. Lennartz, C. Schildknecht and P. Strohhriegl, *Chem. Mater.*, 2010, **22**, 2403–2410.
- 27 J. Ritchie, J. A. Crayston, J. P. J. Markham and I. D. W. Samuel, *J. Mater. Chem.*, 2006, **16**, 1651–1656.
- 28 S. Su, T. Chiba, T. Takeda and J. Kido, *Adv. Mater.*, 2007, **20**, 2125–2130.
- 29 S. A. Vanslyke, C. H. Chen and C. W. Tang, *Appl. Phys. Lett.*, 1996, **69**, 2160–2162.
- 30 Z. Gao, M. Luo, X. Sun, H. Tam, M. Wong, B. Mi, P. Xia, K. Cheah and C. Chen, *Adv. Mater.*, 2009, **21**, 688–692.
- 31 N. Mase, D. Nakamura, Y. Kawano, Y. Suzuki and K. Takabe, *Heterocycles*, 2009, **78**, 3023–3036.
- 32 S. R. Forrest, D. D. C. Bradley and M. E. Thompson, *Adv. Mater.*, 2003, **15**, 1043–1048.
- 33 C. Adachi, R. C. Kwong, P. Djurovich, V. Adamovich, M. A. Baldo, M. E. Thompson and S. R. Forrest, *Appl. Phys. Lett.*, 2001, **79**, 2082–2084.
- 34 R. J. Holmes, S. R. Forrest, Y.-J. Tung, R. C. Kwong, J. J. Brown, S. Garon and M. E. Thompson, *Appl. Phys. Lett.*, 2003, **82**, 2422–2424.
- 35 Y. Agata, H. Shimizu and J. Kido, *Chem. Lett.*, 2007, **36**, 316–317.